Journal of Alloys and Compounds 501 (2010) L29–L32

Contents lists available at ScienceDirect

Journal of Alloys and Compounds

journal homepage: www.elsevier.com/locate/jallcom

Letter

Structural, dielectric and magnetic properties of Pr substituted $Bi_{1-x}Pr_xFeO_3$ $(0 \le x \le 0.15)$ multiferroic compounds

Neeraj Kumar[a], Neeraj Panwar[b], Bhasker Gahtori[a], Neelam Singh[c], H. Kishan[a], V.P.S. Awana[a,*]

[a] National Physical Laboratory (CSIR), Dr. K.S. Krishnan Marg, New Delhi 110012, India
[b] Department of Physics, University of Puerto Rico, San Juan 00931, PR, USA
[c] Department of Physics and Astrophysics, University of Delhi, Delhi 110007, India

ARTICLE INFO

Article history:
Received 24 December 2009
Received in revised form 14 April 2010
Accepted 14 April 2010
Available online 22 April 2010

PACS:
77.65.−j
77.80.−e
75.80.+q
61.05.cp
78.20.−e
75.50.Ee

Keywords:
Multiferroics
Ferroelectricity
Dielectric losses
Ferro/Antiferromagnetism

ABSTRACT

Here we report the structural, dielectric, electric polarization and magnetic properties of $Bi_{1-x}Pr_xFeO_3$ $(0 \le x \le 0.15)$ ceramic compounds. The samples have been synthesized by conventional solid state reaction method at 815 °C and it was observed that they crystallize in the rhombohedral structure. Rietveld refinement was carried out with two possible space groups viz. $R3C$ and $P1$. With an increase in Pr content the dielectric constant increases, whereas the dielectric loss decreases. Pristine and substituted $BiFeO_3$ compounds exhibited substantial ferroelectric polarization at room temperature. An optimum or saturation like scenario was noticed with $x = 0.12$ sample. Isothermal magnetization (M-H) plots of pristine $BiFeO_3$ indicated weak ferromagnetic (FM) character presumably due to the presence of minute $Bi_{25}FeO_{39}$ secondary phase. It is also observed that the magnetic Neel temperature (T_N) increases with increasing Pr content. Interestingly, with Pr substitution at Bi-site the impurity phase tends to disappear and the antiferromagnetic (AFM) nature appears at 300 K.

1. Introduction

Multiferroic compounds exhibiting both magnetic and ferroelectric ordering in the same phase have recently attracted renewed fundamental interest and the coupling between magnetic and ferroelectric degrees of freedom opens up new perspectives in wide technological applications in data storage devices [1,2]. In such materials, magnetization can be induced by the application of electric field and magnetic field can induce electric polarization. However, the temperature at which the coupling between both orderings exists is important from the application viewpoint. One always looks for substantial coupling between them near room temperature. Historically, research on multiferroic materials started in 1960s [3], however, at that time these materials could not attract much attention because single phase materials with more than one ferroic property could not be produced. Recently, many multiferroic materials such as $BiFeO_3$ [4], $CdCr_2S_4$ [5], $LuFe_2O_4$ [6], and $RMnO_3$ [7] have been reported. Among various reported multiferroic materials parent/substituted $BiFeO_3$ (BFO) ceramics and films have so far attracted more interest than others because it exhibits a *G*-type antiferromagnetic (AFM) ordering (T_N) ~370 °C and ferroelectric ordering (T_C) ~830 °C both above room temperature [3,8–10]. Even though BFO is AFM often a weak FM component is observed due to canting of Fe^{3+} spins at room temperature [7]. The spontaneous magnetization can be improved by changing the Fe–O–Fe bond angle or the distribution of mixed Fe ions which in turn, can be achieved either by Bi site substitution or the change in the oxygen content, within the same crystallographic phase [1,4,7]. Recently, Mazumder and Sen reported Pb substituted polycrystalline BFO compound having improved density with superior ferroelectric properties [11]. Li et al. reported weak FM component in AFM ordered state due to oxygen vacancies created by Sr substitution at Bi-site in BFO [12]. In the same line, Catalan et al. argued that one can tune the magnetic ordering temperature as a result of the chemical pressure created by cations substitution [13]. Simoes et al. reported electrical properties of La substituted BFO and observed a decrease in the leakage current density and superior ferroelectric hysteresis loops at room temperature [14]. Wang et al. suggested that La-doping in BFO effectively reduces the concentration of charged defects and dielectric loss [15]. Lee

---

[*] Corresponding author. Tel.: +91 11 45609210; fax: +91 11 45609310.
E-mail address: awana@mail.nplindia.ernet.in (V.P.S. Awana).

0925-8388/$ – see front matter © 2010 Elsevier B.V. All rights reserved.
doi:10.1016/j.jallcom.2010.04.095

et al. reported that La-doping modified the structure of BFO films from the monoclinic to tetragonal state and improved ferroelectric reliability and magnetic properties [16]. Uchida et al. reported that the crystal anisotropy and the Curie temperature of BFO degraded continuously with the increase of La and Nd doping [17]. Hu et al. reported that the Gd-doped BFO films showed a phase transition from rhombohedral to pseudotetragonal structure and no obvious fatigue [18]. Liu et al. observed gradual phase transition from a rhombohedral to a pseudotetragonal structure, low leakage current, square-shaped P-E hysteresis loop with a remanent polarization ($2P_r$) of 143.4 μC/cm^2 and improved anti-fatigue characteristics after 10^{10} read/write polarization cycles in the Ce-doped BFO films [19]. Their films exhibited ferromagnetism also and the saturation magnetization increased with the increase of Ce content. From the aforementioned discussion it is clear that rare-earth ion doping at the Bi-site in BFO compound is beneficial in observing the improved properties as compared to the undoped one.

We have also attempted to study the structural, dielectric, electric polarization and magnetic property Pr-doped BFO ceramic compounds. The reason for choosing Pr is that in the oxide form it exhibits a mixture of +3 and +4 oxidation states which may help in the improvement of the electrical properties due to the suppression of oxygen vacancies. In addition, due to the difference in ionic radii, it is also expected that Pr doping could induce some structural modifications which will eventually affect the electrical and magnetic properties of BFO compound.

2. Experimental

The titular compounds with nominal compositions $Bi_{1-x}Pr_xFeO_3$ ($0 \le x \le 0.15$) have been prepared by conventional solid state reaction method. Stoichiometric ratios of Bi_2O_3, Pr_6O_{11} and Fe_2O_3 (all from Aldrich chemical Ltd. with 99.9% purity) were mixed and ground thoroughly in isopropyl alcohol to get homogeneous mixture and calcined at 815 °C for 10 min in a pre-heated furnace. These calcined mixtures were then pressed into pellets and sintered again in air at 815 °C for 15 min. X-ray diffraction (XRD) patterns were recorded on RIGAKU machine with Cu-Kα radiation (1.54 Å) at a scan rate of 0.5°/min. Dielectric properties were measured using multi-frequency LCR meter whereas ferroelectric polarization (P-E) loops were recorded with a home-made Sawyer-Tower circuit. Magnetic measurements were performed using vibrating sample magnetometer (VSM-Lakeshore).

3. Results and discussion

3.1. Crystal structure:

Fig. 1 shows the XRD patterns of the nominal series $Bi_{1-x}Pr_xFeO_3$ ($0 \le x \le 0.15$) compounds. Some impurity peaks of $Bi_{25}FeO_{39}$ compound can be seen in the parent compound (represented by *), however, with Pr substitution these peaks get disappeared and fewer new peaks are observed which may indicate a structural transition or impurity peaks of Pr_6O_{11}. Room temperature XRD patterns revealed that all these samples exist in rhombohedral as well as triclinic structure. Rhombohedral structure can be described in hexagonal frame of reference with *R*3*C* space group. In hexagonal unit cell Bi/Pr and Fe are located at 6a: (0, 0, 0) and (0, 0, *z*) respectively and O is located at 18b: (*x*, *y*, *z*) [20]. With Pr substitution there is a regular shift towards higher 2θ angle indicating the decrease in the unit cell volume. This can be understood in terms of smaller ionic size of Pr^{3+} (1.12 Å) in comparison to Bi^{3+} (1.17 Å) ion [21]. Besides peak shift, peak intensity also changes with Pr substitution, indicating a possible structural phase transition similar to La substituted BFO compound [22]. Using Fullprof suite programme (1.00)/Reitveld refinement, we calculated the unit cell parameters in *R*3*C* space group. For the parent compound the calculated lattice parameters are 5.578(4) Å, 5.578(4) Å and 13.861(4) Å. Alongwith the pristine sample the lattice parameters for all other Pr substituted samples are listed in Table 1 Table 1. The monotonic change in cell parameters indicates the successful substitution of Pr at Bi-site. Further, we tried to refine the calculated XRD data in the triclinic structure with *P*1 space group [23]. As shown in Fig. 1, the simulated XRD patterns agree well with the measured data. The calculated parameters after refinement in *P*1 space group are listed in Table 2 Table 2. Triclinic structure of $BiFeO_3$ possesses 3.962(4) Å, 3.965(4) Å, and 3.964(4) Å with $\alpha = 89.456$, $\beta = 90.585$, $\gamma = 90.541$. Calculated parameters are slightly larger in comparison to those for the rhombohedral structure i.e. $a = b = c = 3.942$ Å and $\alpha = \beta = \gamma = 89.430$. This may be attributed to the presence of extra $Bi_{25}FeO_{39}$ impurity phase [24]. In a nutshell, we observed that Pr substituted $BiFeO_3$ samples crystallize in reported *R*3*C* and *P*1 space groups with minimal impurities.

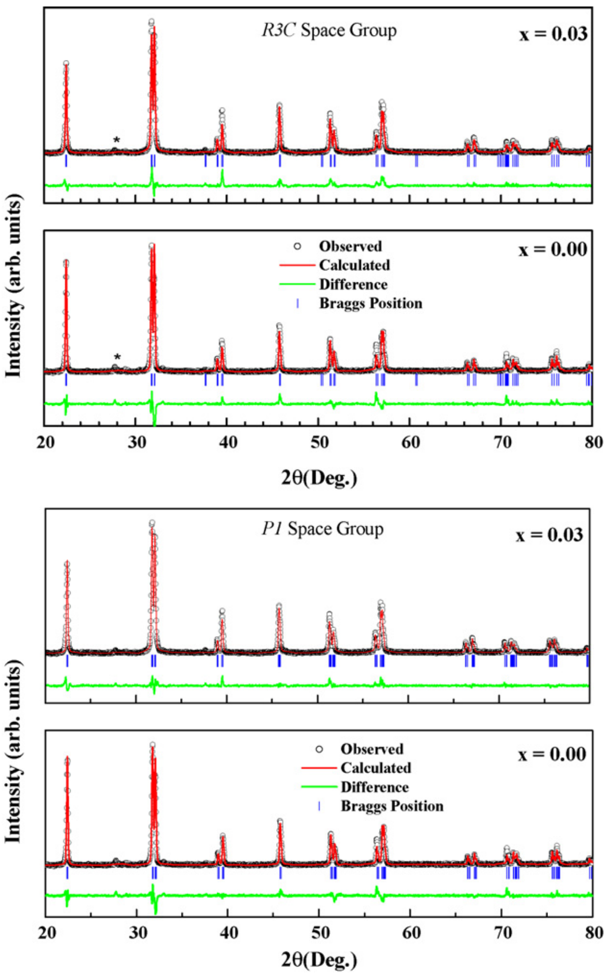

Fig. 1. Reitveld fitted XRD patterns of $Bi_{1-x}Pr_xFeO_3$ ($x = 0.00, 0.03$) samples.

3.2. Dielectric measurements

Jiang and Nan reported the pressure effect on dielectric constant for La substituted $BiFeO_3$ compound and observed that increase in the pressure during the formation of the pellets reduces the

Table 1
Unit cell parameters of $Bi_{1-x}Pr_xFeO_3$ ($0 \le x \le 0.15$) series samples in *R*3*C* space group.

$Bi_{1-x}Pr_xFeO_3$	*a* (Å)	*b* (Å)	*c* (Å)	Volume (Å^3)	χ^2
$x = 0.00$	5.578(4)	5.578(4)	13.861(4)	373.440(4)	3.14
$x = 0.03$	5.577(4)	5.577(4)	13.860(4)	373.315(4)	2.82
$x = 0.06$	5.577(4)	5.577(4)	13.856(4)	373.200(4)	2.90
$x = 0.09$	5.577(4)	5.577(4)	13.853(4)	373.145(4)	2.93
$x = 0.12$	5.576(4)	5.576(4)	13.848(4)	372.915(4)	2.83
$x = 0.15$	5.577(4)	5.577(4)	13.848(4)	373.052(4)	3.10

Table 2
Unit cell parameters of $Bi_{1-x}Pr_xFeO_3$ ($0 \le x \le 0.15$) series samples in $P1$ space group.

$Bi_{1-x}Pr_xFeO_3$	a (Å)	b (Å)	c (Å)	α	β	γ	Volume (Å^3)	χ^2
$x = 0.00$	3.962(4)	3.965(4)	3.964(4)	89.456	90.585	90.541	62.251(4)	3.28
$x = 0.03$	3.960(4)	3.963(4)	3.965(4)	89.453	90.528	90.562	62.227(4)	2.86
$x = 0.06$	3.959(4)	3.963(4)	3.965(4)	89.464	90.575	90.531	62.201(4)	2.96
$x = 0.09$	3.958(4)	3.962(4)	3.966(4)	89.456	90.537	90.585	62.178(4)	2.89
$x = 0.12$	3.956(4)	3.962(4)	3.965(4)	89.475	90.528	90.581	62.132(4)	2.86
$x = 0.15$	3.954(4)	3.962(4)	3.966(4)	89.486	90.476	90.588	62.134(4)	3.30

change in oxygen content [25]. Wang et al. reported that slow heating and long sintering time encouraged the oxygen inhomogeneity [2]. Therefore, to reduce the possibility of fluctuation in oxygen stoichiometry and its repercussion on the dielectric behaviour we chose rapid synthesis method using a pre-heated furnace. Figs. 2 and 3 show the dielectric behaviour of the series $Bi_{1-x}Pr_xFeO_3$ ($0 \le x \le 0.15$). The real and imaginary parts of dielectric constant increase along with a decrease in the dielectric loss with Pr substitution. For $x = 0.09$ sample the dielectric loss is maximum in the low frequency regime and for $x = 0.06$, 0.12, 0.15, the same is minimum and invariant in the high frequency range. Higher losses in these materials generally represent large leakage current due to higher conductivity. A decrease in the value of dielectric loss for doped samples suggests that Pr substitution is helpful in reducing the leakage current.

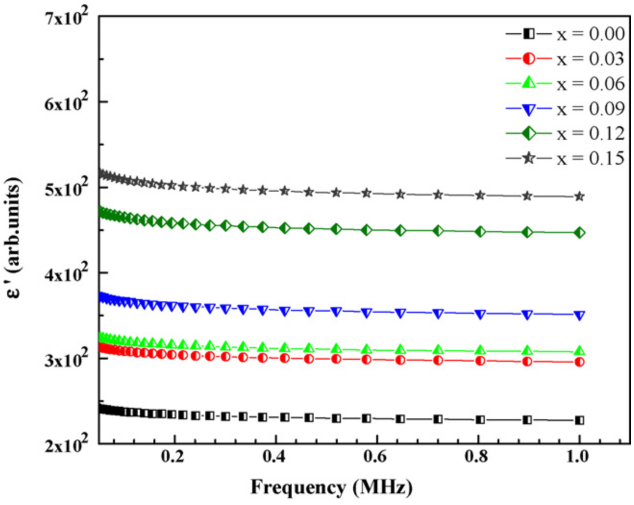

Fig. 2. Variation of ε' with frequency for the series $Bi_{1-x}Pr_xFeO_3$ ($0 \le x \le 0.15$) samples.

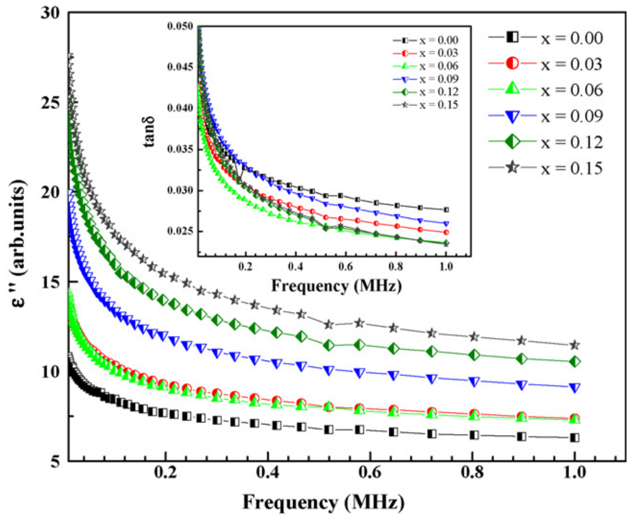

Fig. 3. Variation of ε'' with frequency for the series $Bi_{1-x}Pr_xFeO_3$ ($0 \le x \le 0.15$) samples. Inset shows the variation of tan δ for $Bi_{1-x}Pr_xFeO_3$ ($0 \le x \le 0.15$).

Fig. 4 exhibits the ferroelectric hysteresis loop measured for $Bi_{1-x}Pr_xFeO_3$ ($0 \le x \le 0.15$) at room temperature. The compounds were polarized four times by repeated electric field. The entire series show a linear loosy and unsaturated loop. With Pr substitution, there is an increase in observed saturation polarization (P_s), remnant polarization (P_r) and coercive field (E_c). In case of pristine compound BFO, P_s reaches 0.186 μC/cm^2 (applied field of 11.237 kV/cm) with remnant polarization (P_r) 0.086 μC/cm^2 and coercive field (E_c) 4.85 kV/cm. For $x = 0.15$ Pr substituted sample these values enhanced upto 0.223 μC/cm^2 (applied field of 15.311 kV/cm), 0.101 μC/cm^2 and 6.861 kV/cm respectively. Therefore, one can notice that with Pr substitution in BFO there is an apparent increase in P_s, P_r and E_c values.

3.3. Magnetic measurements

Fig. 5 shows the room temperature magnetization (M-H) plots for the $Bi_{1-x}Pr_xFeO_3$ ($0 \le x \le 0.15$). All the samples show magnetic hysteresis loops representing weak ferromagnetic (FM) behaviour. The FM component is more visible for pristine sample and lesser for Pr substituted samples. The parent compound is reported to be a G-type antiferromagnetic at room temperature [3]. At the same time, there are several reports that show the FM like magnetic hysteresis in pure $BiFeO_3$ compound [11,12], however, this is not a universal phenomenon [2,3]. It is, therefore, questionable whether the room temperature weak FM character is intrinsic magnetic property of $BiFeO_3$ or extrinsic. The possible impurities may be γ-Fe_2O_3 or Fe_3O_4. The observed coercivity for γ-Fe_2O_3 and Fe_3O_4 are 450 Oe, 25 Oe respectively [26]. In the present study, for the parent compound the calculated coercivity is about 56 Oe. The observed value lies between those of γ-Fe_2O_3 and Fe_3O_4 ruling

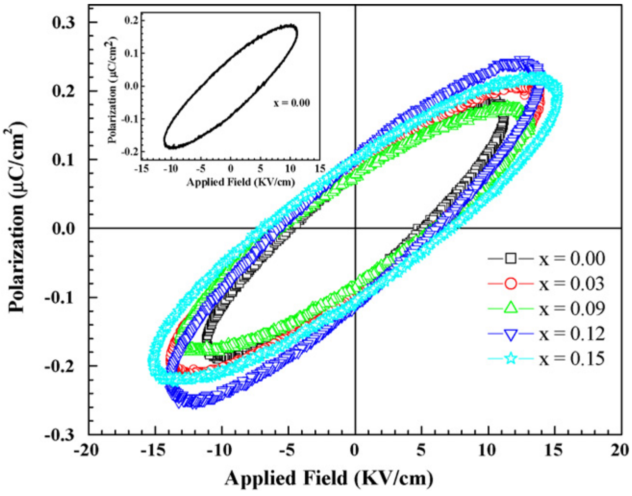

Fig. 4. Polarization variation with applied field of $Bi_{1-x}Pr_xFeO_3$ ($0 \le x \le 0.15$) series at room temperature.

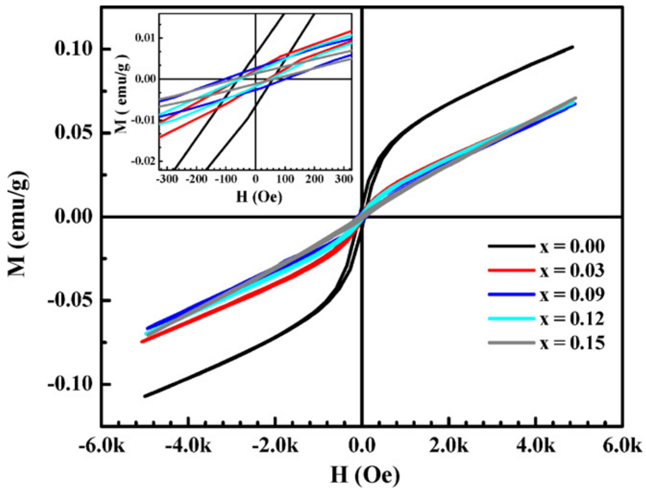

Fig. 5. Magnetization variation with applied magnetic field of $Bi_{1-x}Pr_xFeO_3$ ($0 \leq x \leq 0.15$) series at room temperature.

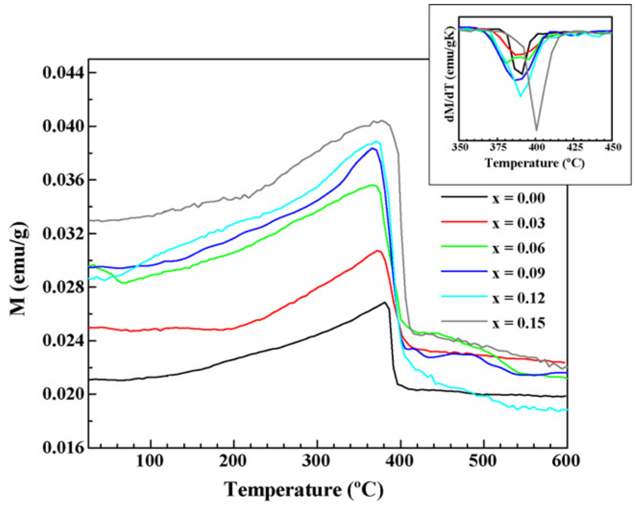

Fig. 6. Magnetization variation with temperature of the $Bi_{1-x}Pr_xFeO_3$ ($0 \leq x \leq 0.15$) series.

out their presence as secondary phases. Other possibility is the presence of $Bi_{25}FeO_{39}$ phase [24] which is confirmed by XRD patterns and indicated by * in Fig. 1. With Pr substitution $Bi_{25}FeO_{39}$ impurity phase gets suppressed and as a result of this the coercivity and remnant magnetization being observed in M-H loops decreased substantially. These results revealed that Pr substitution in $BiFeO_3$ not only improves the electric polarization parameters (P_s, P_r and E_c) but also diminishes the often observed $Bi_{25}FeO_{39}$ impurity phase responsible for FM contribution in the parent BFO compound. Hence, in higher Pr substituted samples the magnetic hysteresis loops exhibit near linear field dependence the natural antiferromagnetic behaviour of $BiFeO_3$ [3].

Fig. 6 shows the temperature dependent magnetization of Pr substituted BFO samples. With increasing Pr substitution the antiferromagnetic transition temperature (T_N) increases and for $x = 0.15$ sample it is 400 °C (T_N calculated from dM/dT vs. T plots and shown in the inset of Fig. 6). It is observed that T_N increases with Pr content. Recently, Catalan et al. measured an increase in T_N ~0.6–0.66 K/mol-Ca content in Ca-substituted BFO samples [13]. Since Ca (1.17 Å) and Pr ions have nearly same ionic radii (1.12 Å), thus both ions seem to have equal chemical pressure in lattice structure. As we increase Pr content, the lattice volume decreases and the overlapping Fe-orbitals in Fe–O–Fe bond increases. Eventually, this leads to the enhancement of the antiferromagnetic superexchange and thus increasing the Neel temperature. The Neel temperature of BFO system increases at a rate of 2.2 K/GPa under hydrostatic pressure [13]. On comparing these one can notice that 1 mole Pr substitution is equivalent to 0.32 GPa hydrostatic pressure. Based on these, it is suggested that with Pr substitution in BFO compound can control magnetic character/T_N in a similar way as the application of hydrostatic pressure.

4. Conclusions

We have successfully synthesized Pr substituted $BiFeO_3$ compounds. All the samples can be fitted in both rhombohedral $R3C$ and triclinic $P1$ space groups. Pr substitution decreases the volume of unit cell due to its smaller ionic size. Further with Pr substitution impurity phase $Bi_{25}FeO_{39}$ reduces and there is a decrease in the dielectric loss as well. Increase in the dielectric constant is observed for doped $BiFeO_3$. Higher polarization is observed for the Pr substituted systems with an increase in remnant polarization (P_r) and coercive field (E_c). Field and temperature dependent magnetization behaviour support the presence of $Bi_{25}FeO_{39}$ in pure BFO and increase in the Neel temperature is also observed with Pr content.

Acknowledgement

One of the authors (N. K.) is thankful to the Council of Scientific and Industrial Research (CSIR), India for providing the Senior Research Fellowship (SRF).

References

[1] G. Catalan, J.F. Scott, Adv. Mater. 21 (2009) 2463.
[2] Y.P. Wang, L. Zhou, X.Y. Chen, J.M. Liu, Z.G. Liu, Appl. Phys. Lett. 84 (2000) 855.
[3] G.A. Smolenskii, V.M. Yudin, Sov. Phys. – Solid State 6 (1965) 2936.
[4] J. Wang, J.B. Neaton, H. Zheng, V. Nagarajan, S.B. Ogale, B. Liu, D. Viehland, V. Vaithyanathan, D.G. Schlom, U.V. Waghmare, N.A. Spaldin, K.M. Rabe, M. Wuttig, R. Ramesh, Science 299 (2003) 1719.
[5] J. Hemberger, P. Lunkenheimer, R. Fichhtl, H.A.K. Von Nidda, V. Tsurkan, A. Loidl, Nature 434 (2005) 364.
[6] N. Ikeda, H. Ohsumi, K. Ohwada, K. Ishii, T. Inami, K. Kakurai, Y. Murakami, Y. Yoshii, S. Mori, Y. Horribe, H. Kito, Nature 436 (2005) 1136.
[7] N. Hur, S. Park, P.A. Sharma, J.S. Ahn, S. Guha, S.W. Cheong, Nature 429 (2004) 392.
[8] A.Z. Simoes, R.F. Pianno, E.C. Aguiar, E. Longo, J.A. Varela, J. Alloys Compd. 479 (2009) 274.
[9] M.B. Bellakki, V. Manivannan, J. Sol-Gel Sci. Technol. 53 (2010) 184.
[10] J.H. Xu, H. Ke, D.C. Jia, W. Wang, y. Zhou, J. Alloys Compd. 472 (2009) 473.
[11] R. Mazumder, A. Sen, J. Alloys Compd. 475 (2009) 577.
[12] J. Li, Y. Duan, H. He, D. Song, J. Alloys Compd. 315 (2001) 259.
[13] G. Catalan, K. Sardar, N.S. Church, J.F. Scott, R.J. Harrison, S.A.T. Redfern, Phys. Rev. B 79 (2009) 212415.
[14] A.Z. Simoes, F.G. Garcia, C. d. S. Riccardi, J. Mater. Chem. Phys. 116 (2009) 305.
[15] Y. Wang, R.Y. Zheng, C.H. Sim, J. Wang, J. Appl. Phys. 105 (2009) 016106.
[16] D. Lee, M.G. Kim, S. Ryu, H.M. Jang, Appl. Phys. Lett. 86 (2005) 222903.
[17] H. Uchida, R. Ueno, H. Funakubo, S. Koda, J. Appl. Phys. 100 (2006) 014106.
[18] G.D. Hu, X. Cheng, W.B. Wu, C.H. Yang, Appl. Phys. Lett. 91 (2007) 232909.
[19] J. Liu, M. Li, L. Pei, J. Wang, B. Yu, X. Wang, X. Zhao, J. Alloys Compd. 493 (2010) 544.
[20] K.D. Rouse, M.J. Cooper, Acta Crystallogr. 26 (1970) 682.
[21] R.D. Shanon, Acta Crystallogr. A 32 (1976) 751.
[22] A.V. Zalesskii, A.A. Frolov, T.A. Khimich, A.A. Bush, Phys. Solid State 45 (2003) 141.
[23] Y.P. Wang, L. Zhou, M.F. Zhang, X.Y. Chen, J.M. Liu, Z.G. Liu, Appl. Phys. Lett. 84 (2004) 1731.
[24] D. Lebeugle, D. Colson, A. Forget, M. Viret, P. Bonville, J.F. Marucco, S. Fusil, Phys. Rev. B 76 (2007) 024116.
[25] Q.H. Jiang, C.W. Nan, J. Am. Ceram. Soc. 89 (2006) 2123.
[26] R.C.O. Handley, Modern Magnetic Materials: Principles and Applications, Wiley, New York, 2000.